Microtexture Performance of EAF Slags Used as Aggregate in Asphalt Mixes: A Comparative Study with Surface Properties of Natural Stones

Rosolino Vaiana *[ID], Filippo Balzano, Teresa Iuele and Vincenzo Gallelli

Department of Civil Engineering, University of Calabria, 87036 Rende, Italy
* Correspondence: rosolino.vaiana@unical.it; Tel.: +39-0984-496786

check for updates

Abstract: Steelmaking industries produce a large amount of solid wastes that need to be adequately managed in order to ensure environmental sustainability and reduce the impact of their disposal on earth pollution. Electric arc furnace (EAF) slags are those wastes deriving from secondary steelmaking production; these slags can be re-used and recycled in many industrial applications such as the production of asphalt mixes. In this paper authors investigate the surface performance of EAF slags used as second-hand aggregate in asphalt mixes. In particular, slags behavior under polishing is compared to other types of aggregate commonly used for asphalt concrete such as limestone, basalt, and kinginzite. Several devices (skid tester, laser profilometer, polishing machine) were used to collect experimental data; the analysis of microtexture was carried out by comparing aggregate surface performance before and after polishing. Results show that EAF slags are positively comparable to basalt as concerns the polishing behavior; good correlations between skid resistance and some microtexture indicators are also carried out.

Keywords: EAF slags; steelmaking industry; aggregate microtexture; asphalt mixes

1. Introduction

Metallurgical industry is one of the world's largest contributors to the anthropogenic CO_2 emissions. Until the last years of 19th century, most of the produced steel derived from the integrated process (blast furnace, BF/basic oxygen furnace, BOF route) used coal as the reducing agent and iron as raw material [1]. Nowadays, in order to reduce energy consumption and bring CO_2 emissions close to zero, a secondary production route using an electric arc furnace (EAF) is becoming far more widespread. According to previous researches, by 2060, the share of secondary steel production will exceed the share of the primary one. In the secondary steelmaking process electricity is used to melt iron scraps with chemical additives into steel. Even if the secondary production route requires 56% less energy than the primary one (Institute of Scrap Recycling Industries 2012), a large amount of solid waste materials are produced [2]. As estimated in Steel Industry By-Products Project group report 2007–2009 by World Steel, the average production of 1 ton of steel results in about 200 kg (EAF) to 800 kg (BF/BOF) of solid wastes globally [3]; other studies show that the amount of wastes is 100–180 kg and 200–400 kg for each ton of liquid steel for EAF and BF respectively [4].

In the light of the above, the management of this kind of wastes is becoming a crucial issue especially for the countries with the largest annual production such as India (29 million tons [5]), China (90 million tons [6]), Europe (21 million tons [7]). Therefore, reusing, recycling, and recovering steel wastes in many other industrial applications is extremely important. They are found to be useful in many fields, such as constructions, asphalt concrete, agricultural fertilizer, and for soil improvement. However, better utilization for value-added purposes can be achieved [8,9].

Among industrial wastes, the EAF slags have good physical, chemical, and mechanical characteristics and their use in the construction industry is increased in the last years. Analyzing their intrinsic properties such as granules size, specific weight, or porosity, EAF slags can be considered similar to stone aggregates commonly used in construction engineering [10,11]. This is due to the high iron content, which gives to the EAF slags a hard and wear-resistant constitution. The chemical composition of EAF slags is shown in Table 1 [6].

Table 1. Chemical composition of electric arc furnace (EAF) slags (wt. %) values averaged from [2] by literature analysis.

Chemical Composition	Average Range (%)
SiO_2	5–40
FeO	1.2–50
CaO	15–54
MgO	1–21.4
Al_2O_3	1–15
Others	0.05–5

Although this composition is slightly different in relation to the kind of scraps and additives used, the high levels of FeO and CaO determine the need to carry out special treatments on the raw slags before their use as aggregate. In fact, when free CaO comes in contact with water, it hydrolyzes ($CaO + H_2O \rightarrow Ca(OH)_2$), and its volume duplicates; $Ca(OH)_2$ is a cementitious material resulting in the fine particles cemented on the slag surface, thus compromising the formation of an embedded concrete structure [10,12]. Previous researches [13,14] show that a proper stabilization treatment of EAF slags by exposing them to outdoor weather and regular spraying for at least 90 days may avoid any expansive phenomenon, allowing a safe use of such slag as aggregate in concrete production. Furthermore, the fine powder covered on the slag surface after crushing needs to be removed in order to have edged shaped granules. Steelmaking slags also contain a high amount of iron oxide (FeO) that may lead to corrosion. Therefore, these wastes need an "iron-removal" process by means of a permanent magnetic separator [12,15] for their adequate use in other engineering applications.

After the abovementioned and other specific treatments, EAF slags have generally excellent stone-like mechanical properties. In the last years, many studies have been performed to determine the steelmaking slags suitability for using as aggregate in concrete in order to enhance the "4R—reduce, reuse, recycle, and renew strategy" and optimize the wastes management process for both environmental sustainability and cost savings in steel production [16].

Besides their use in concrete, steelmaking wastes addition to hot mix asphalt for road construction is growing year by year. Several studies have been conducted to test EAF slags performance as aggregate in asphalt concrete for pavement surface layers [11,13]. In addition to adequate mechanical characteristics, steelmaking slags for asphalt mixes must have other suitable features related to aggregate shape, surface roughness, and texture in order to enhance the adherence and skid resistance of pavement surface layers.

Adherence is the tangential force mutually exchanged on the contact surface between tire and road pavement. This phenomenon is related to many aspects including the geometrical characteristics of the micro- or macro-texture of aggregates [17]. Therefore, in order to achieve the goal of enhancing road safety it is important to evaluate the texture performance of steelmaking wastes when used as an aggregate in asphalt concrete. In particular, pavement skid resistance is strictly related to the surface texture, especially in wet conditions; consequently, the accident rate depends both on texture and friction [18–20].

More specifically, road pavements contribute to friction through a combination of micro- and macrotexture. At low speed, microtexture determines the adhesion phenomenon due to the molecular interaction forces which grow between the tire and the surface. At higher speeds the hysteresis mechanism arises: the tire repeatedly deforms, enveloping surface texture asperities [21–24].

Macrotexture determines the hysteretic deformation of the rubber and the consequent development of horizontal forces which are opposed to the slipping of wheels. Surface texture can be supposed to be the superposition of "many" elementary components (harmonics); in particular, macro-texture is related to wavelengths (λ) between 0.5 mm and 50 mm, whereas micro-texture refers to $\lambda < 0.5$ mm [25]. Referring to the micro-texture range, surface polishing phenomenon is also a crucial issue to be investigated. In fact, surface texture and, consequently, skid resistance change over time because of many deterioration phenomena under traffic loadings related to the polishing process of aggregates.

In the light of the above, this paper focuses on the evaluation of EAF slags usability as aggregate in asphalt concrete. In particular, the research is aims to analyze these type of "second-hand aggregate" in relation to durability, wear resistance, and polishing behavior by investigating the relationship between pavement friction and aggregates micro-texture. The EAF slag used in this study is obtained through intense oxygen injection procedures and a subsequent controlled and accelerated cooling with water spray for its complete stabilization.

2. Materials and Methods

For the case study, three types of aggregates commonly used in road pavement were selected: (i) Criggion green basalt coming from Northern Scotland (ID: R); (ii) kinginzite obtained from a stone quarry located in Maida-CZ, Italy (ID: K); (iii) Grey limestone from Amantea-CS, Italy (ID: C) as shown in Figure 1. Moreover, EAF slags coming from the "Ferriere Nord—Gruppo Pittini" steelmaking industry (Potenza, Italy) were analyzed (identified as ID: A sample in the following). Main mechanical properties of all aggregates are shown in Table 2.
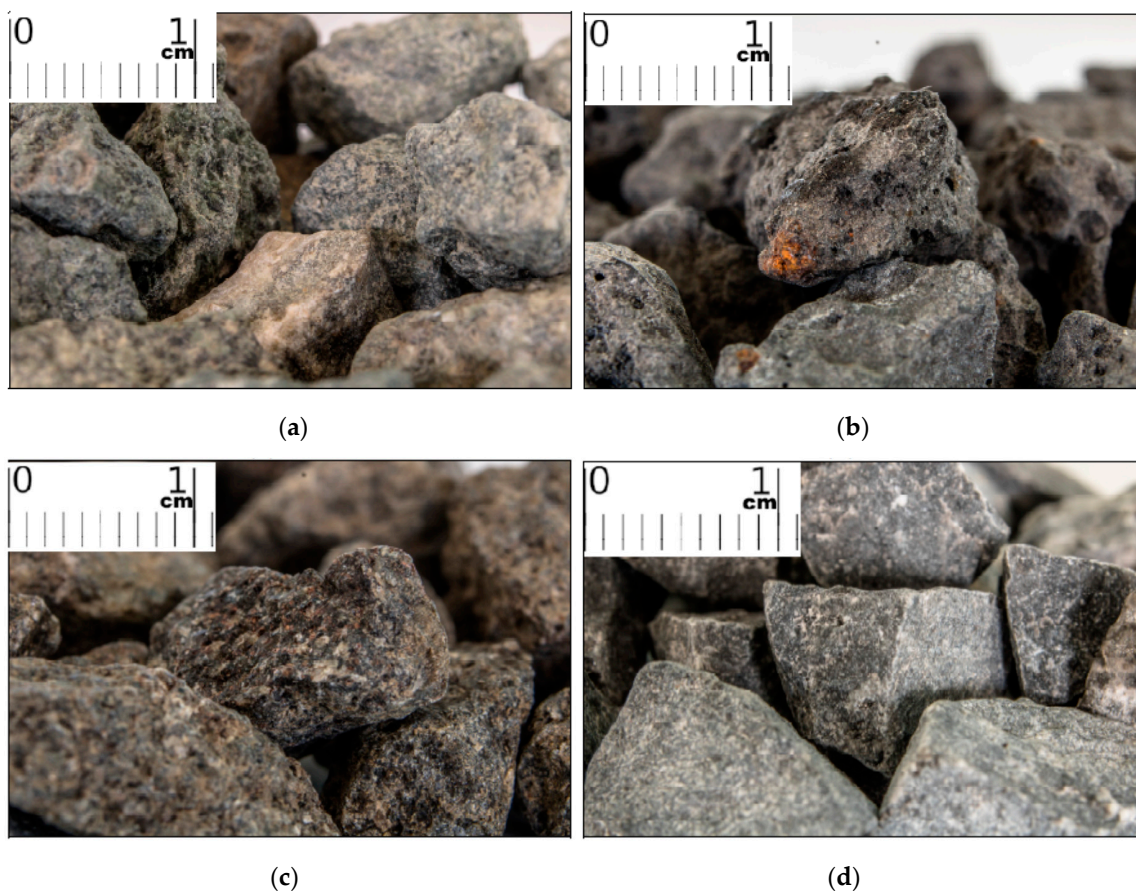

(a)

(b)

(c)

(d)

Figure 1. Selected aggregates: (**a**) Basalt (ID: R); (**b**) EAF slags (ID: A); (**c**) kinginzite (ID: K); (**d**) limestone (ID: C).

Table 2. Main mechanical properties of aggregates.

Test	Standards	Basalt (ID: R)	EAF Slags (ID: A)	Kinginzite (ID: K)	Limestone (ID: C)
Los Angeles	UNIEN 1097-2	14	15	23	22
Micro Deval	UNIEN 1097-1	9	10	19	16

The first step of the experimental plan was the selection of aggregates with a specific stone dimension (7.2–10 mm), according to the UNI EN 1097/8 2001. Standardized specimens (90.6 mm × 44.5 mm × 12.5 mm) were prepared using a metallic mold. The granules were manually placed over the mold surface in a single layer in order to have from 36 to 46 granules for each specimen, placing the flat surface of each stone externally. Finally, the mold was filled with a bicomponent fiberglass and closed with a shaped cover in order to obtain rigid and non-deformable samples once hardened. Three specimens for each kind of aggregate were realized for a total of 12 samples.

Two longitudinal and three crosswise sections were identified on each specimen by means of a preset mask to carry out profilometric analysis of stone surface texture by means of a laser profilometer based on conoscopic olography before and after polishing (see Figures 2 and 3). Profiles were traced by using a lens with an objective focal length of 50 mm and a sampling resolution of 5 µmm (20 points per millimeter on each profile) [26,27]. This procedure was carried out in order to focus the investigation on PSV tire/test specimen interface (PSV, polished stone value according to the UNI EN 1097/8 2001, see Section 2.2).
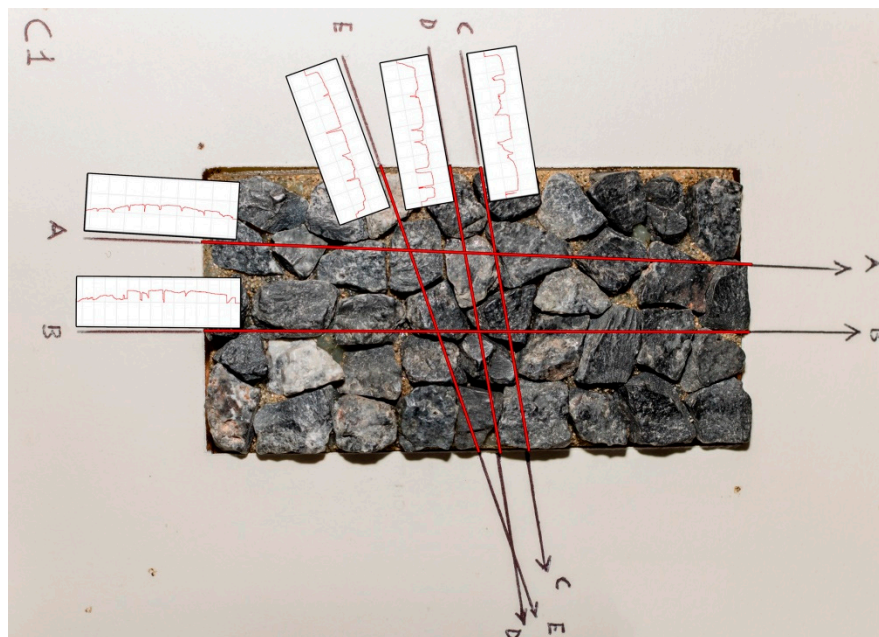

Figure 2. Specimen equipped with preset mask by profilometric alignments (longitudinal A-A, B-B; and crosswise C-C, D-D, E-E) for surface texture investigation.
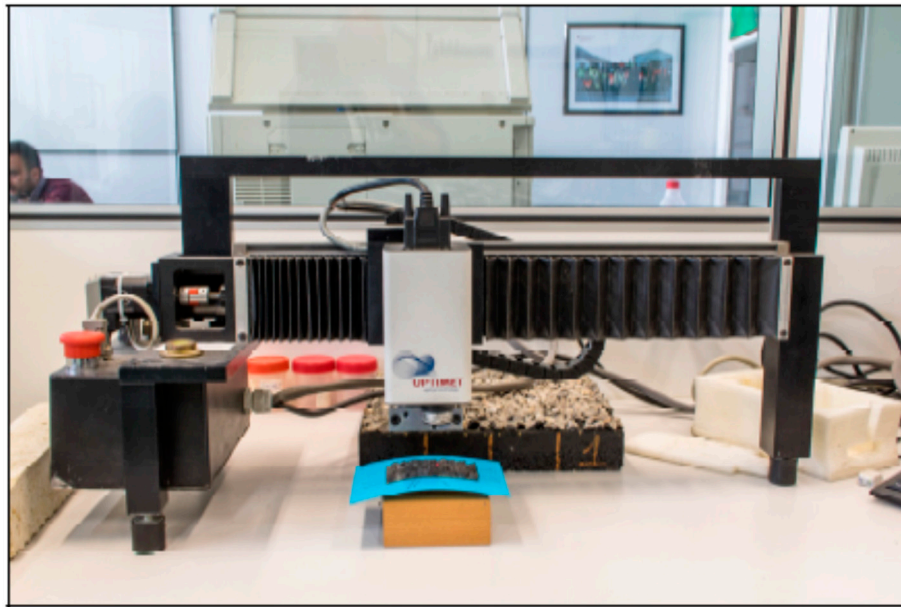
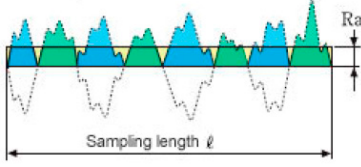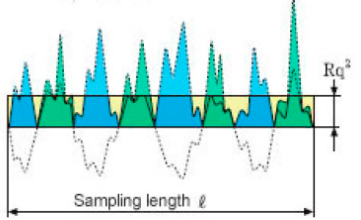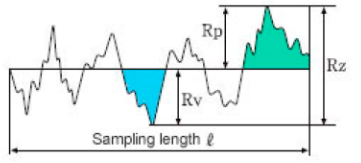**Figure 3.** Contactless laser profilometer.

2.1. Roughness Data Collection

The typical peaks of aggregate surface were visually detected for each profile and sample in order to estimate the microtexture data for all samples. A reference measuring length of about 1 mm was selected and regular slope segments were graphically built on the profile of each aggregate, thus excluding the intergranular macro-valleys from calculations.

Three microtexture aggregate descriptors [26] were estimated: (i) R_A—average roughness or center-line average, that is the arithmetic average of the absolute values of the profile height deviations from the mean line, recorded within the evaluation length; (ii) R_Q—root mean square roughness; (iii) R_Z—average peak-to-valley height. The analytical description of each indicator, together with a graphical representation, is shown in Table 3 [26,28,29].

A total approximately of 12,600 values were collected to calculate the average roughness parameters (before and after polishing): (i) measures on aggregates belonging to the same longitudinal (around 200) and crosswise profile (around 150); (ii) all profiles on each specimen (around 350); (iii) all specimens (12). Furthermore, data referring to all longitudinal and crosswise profiles on each sample were also averaged in order to obtain two different values in relation to the profile direction. Data derived from the analysis of profiles on unpolished aggregates were then compared to those collected after polishing [25,29–32].

Table 3. Investigated roughness parameters.

Roughness Parameter	Formula	Graphical Representation
R_A	$R_A = \frac{1}{n} \sum\limits_{i=1}^{n} \lvert y_i \rvert$	
R_Q	$R_Q = \sqrt{\frac{1}{n} \cdot \sum\limits_{i=1}^{n} y_i{}^2}$	
R_Z	$R_Z = \frac{1}{5} \sum\limits_{i=1}^{5} R_{pi} - R_{vi}$	

2.2. Accelerated Polishing Process

In order to evaluate the behavior of each type of aggregate under polishing, an accelerated polishing machine (Figure 4) was used. Specimens were placed on a rotating wheel that is 406 mm in diameter. The wheel holds the test specimens and two stone control specimens around its rim, thus forming a 44.5 mm wide aggregate surface (UNI EN 1097/8 2001). Overall, 14 specimens were placed around the wheel by the following positioning order:

$$U2 - K3 - A1 - R1 - C1 - K1 - A3 - U1 - C3 - A2 - R2 - C2 - K2 - R3 \tag{1}$$

where U1 and U2 are control specimens that were not considered for PSV calculation but for filling-in of the rotating wheel (UNI EN 1097/8 2001).

(**a**)	(**b**)

Figure 4. Accelerated polishing machine: (**a**) revolving wheel; (**b**) polishing tire-wheel by corn emery.

Each specimen was marked with an arrow indicating the profilometer reading direction during the microtexture analysis and placed by matching this direction and the wheel rotation direction.

The rubber-tired wheel exerts a contact force of 725 N ± 10 N on the molds. For the first 3 h of the test, corn emery is fed onto the wheel at a rate of 27 ± 7 g/min together with a sufficient amount of water. At the end of this first testing cycle, the machine is disassembled and carefully cleaned by water to remove the emery. Afterward, the wheel is relocated on the machine and the test is repeated for other 3 h using flour emery at a rate of 3 ± 1 g/min with the rate of water approximately twice that of the emery flour.

For the experimental investigation, both first and second cycles were performed in a controlled temperature room (20 ± 5 °C). At the end of the second cycle, all specimens were checked to exclude lesions or missing granules. Finally, test specimens were brushed to remove powders and placed for drying over at 25 °C for 24 h to remove residual interstitial moisture.

Following the alignment points previously marked on, all specimens were rescanned using the contactless laser profilometer. Following this procedure, it was possible to record roughness data after polishing on the same directions previously detected on the unpolished samples, with acceptable approximation.

2.3. British Pendulum Tester

Together with the microtexture investigation, all specimens were tested for skid resistance before and after polishing by the British pendulum friction tester. Experimental samples were previously dipped in distilled water at 20 °C for 120 min and then they were placed one by one inside a dedicated block on the base plate of the tester (Figure 5b) after calibrating the instrument in order to have a sliding length of 76 mm for each measurement. To ensure uniform conditions, specimens were regularly spayed with distilled water at 20 °C during the entire test. Each specimen was tested until reaching five regular values on the "F Scale" of the instrument. The last three measurements were averaged to estimate the British pendulum number (BPN).
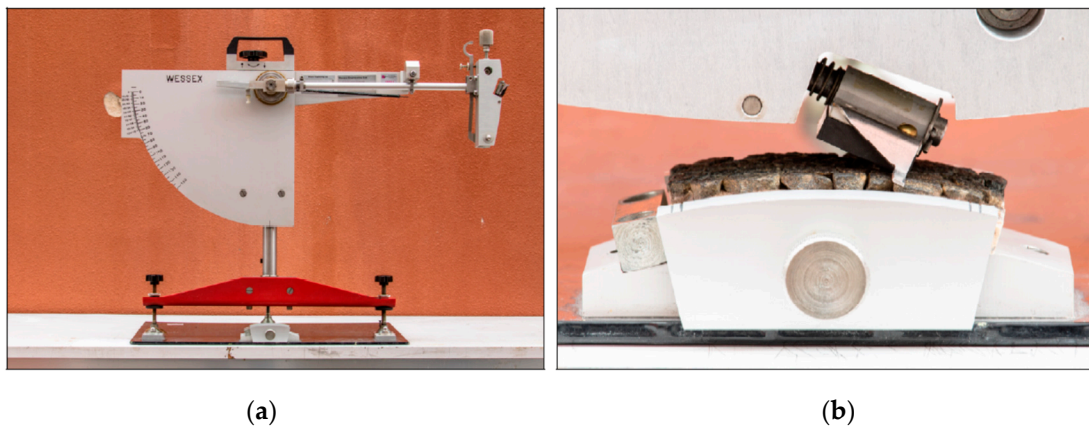

(**a**)　　　　　　　　　　　　　　　　　　　　　　　　(**b**)

Figure 5. (**a**) British pendulum skid tester; (**b**) specimen block on the base plate.

3. Results

3.1. Polished Stone Value (PSV)

To assess the quality of EAF slags as aggregates in asphalt mixes production, skid resistance measurements on the polished specimens were used to derive PSV. According to the UNI EN 13036/4, the PSV was determined using the following equation:

$$PSV = S + (52.5) - D \tag{2}$$

where S is the mean value of skid resistance for the aggregate test specimens and D is the mean value of skid resistance for the PSV control stone specimens. By considering basalt as control aggregate, this last value was 55.7, as shown in Table 4.

Table 4. Polished stone value results for the examined aggregates.

Average Value of Control Stone	D	55.7			
		Basalt	EAF Slags	Kinzigite	Limestone
Average Value of Aggregate	**S**	55.7	55.0	49.3	39.3
Polished Stone Value	**PSV**	52.5	51.8	46.2	36.2
Threshold Values [33]	**PSV**			$\geq$44	

Starting from the data summarized in Table 4, it is possible to highlight a first result: The polished stone value registered for EAF slags samples is comparable to one of the control aggregate. Furthermore, it is upper at requirement values set by main Italian Highways Agency [33].

3.2. Skid Resistance

Friction results are shown in Table 5, where BPN * is the British pendulum value measured on samples before polishing, whereas BPN refers to the measurements registered on polished aggregates. Furthermore, the percentage variation between the two measurements (BPN and BPN *, respectively) was calculated for each specimen and for all specimens with the same aggregate (see ΔBPN in Table 5 and average ΔBPN in Figure 6). As it is possible to see, slags behavior is quite similar to that registered for basalt aggregate: The percentage variation of friction before/after polishing has values from -5.4% to -8.9% with an average value of about -7%. For kinginzite and limestone samples double (-14%) and three (-21%) times higher results were registered, thus highlighting a great decrease of the available surface friction under traffic loadings.

Table 5. British pendulum skid resistance test results.

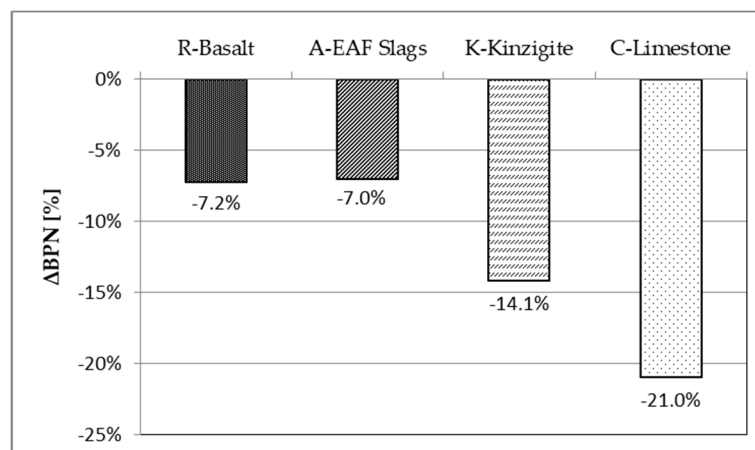| Specimen	R1	R2	R3	A1	A2	A3	K1	K2	K3	C1	C2	C3
	Basalt			EAF Slags			Kinzigite			Limestone		
BPN *	62.0	60.0	58.8	62.0	57.3	58.0	58.7	58.0	55.7	47.3	50.0	52.0
BPN	57.7	54.7	54.7	58.7	53.3	53.0	50.0	50.0	48.0	38.0	38.0	42.0
$\Delta BPN = 100 \cdot \frac{BPN - BPN\,^*}{BPN\,^*}$	-7.0	-8.9	-5.7	-5.4	-7.0	-8.6	-14.8	-13.8	-13.8	-19.7	-24.0	-19.2

Figure 6. Average ΔBPN% (British Pendulum Number) for each aggregate after the accelerated polishing process.

3.3. Roughness Data Analysis

Microtexure data were collected on all samples for both unpolished (R_A *, R_Q *, R_Z *) and polished (R_A, R_Q, R_Z) conditions. Table 6 summarizes the final roughness values estimated by averaging all longitudinal and crosswise profiles on each sample for a total of about 350 readings for both polishing conditions.

Table 6. Roughness data collected by profilometric analysis (baseline length $\approx$ 200 µm).

Samples/Microtexture	Before (µm)			After (µm)			Variation (%)		
	R_A *	R_Q *	R_Z *	R_A	R_Q	R_Z	ΔR_A	ΔR_Q	ΔR_Z
R1	12.54	16.07	35.37	11.82	15.08	33.43	−6.15	−6.56	−5.78
R2	11.92	15.03	34.48	11.23	14.16	32.27	−6.19	−6.13	−6.85
R3	11.86	14.98	35.18	11.26	14.20	33.29	5.38	5.49	5.68
A1	10.89	14.02	31.63	10.42	13.69	30.24	−4.49	−2.40	−4.59
A2	11.19	14.27	31.58	10.45	13.29	29.75	−7.13	−7.38	−6.13
A3	10.85	13.73	32.13	10.35	13.23	30.25	−4.76	−3.76	−6.22
K1	15.03	19.09	43.60	13.60	17.29	39.55	−10.54	−10.39	−10.24
K2	12.74	16.38	39.25	11.74	15.01	35.81	−8.59	−9.17	−9.61
K3	11.74	14.91	34.70	10.93	13.77	31.62	−7.41	−8.26	−9.74
C1	9.87	12.24	28.50	8.35	10.34	23.98	−18.17	−18.31	−18.86
C2	9.09	11.45	26.63	7.65	9.49	22.12	−18.81	−20.68	−20.16
C3	9.305	11.65	26.86	8.04	10.05	22.71	−15.69	−15.88	−18.29

The microtexture indicators marked with (*) refer to the measurements performed before polishing test.

Roughness data variation was calculated as the percentage difference between the values registered before and after polishing, as for BPN results.

$$\Delta R_i = \frac{R_i - R_i^*}{R_i^*} \times 100 \tag{3}$$

The abovementioned ΔR_i (with $i = a, q, z$) can be evaluated as a parameter that quantifies aggregate surface evolution due to polishing. The average values estimated for each type of aggregate are shown in Figure 7.
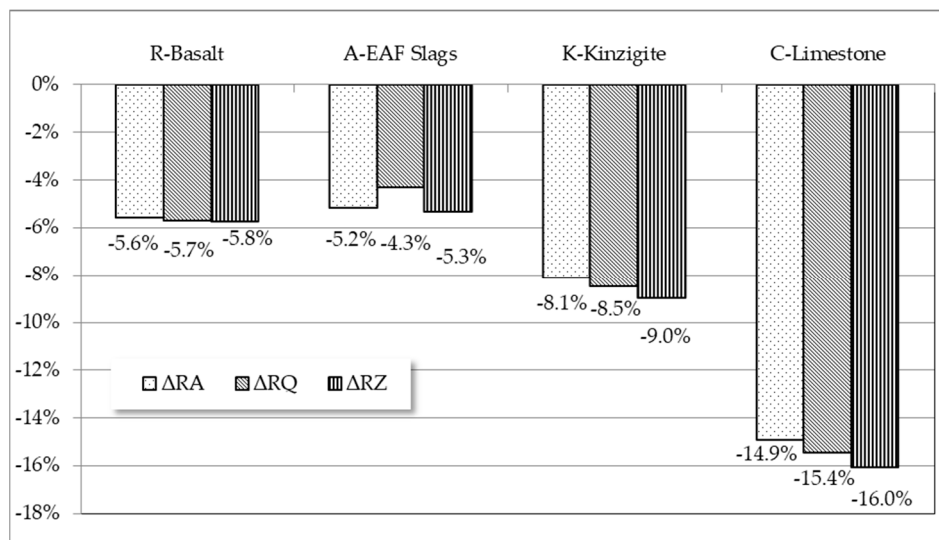

Figure 7. Average ΔR_i for each aggregate after polishing.

As it is possible to see in Figure 7, percentage variations are all higher than 5%. In particular, the greatest differences of microtexture before/after polishing were registered for kinginzite (ΔRi from −8.1% to −9%) and limestone (ΔRi from −14.9% to −16%). An essentially unchanged micro-peaks configuration surface was observed for basalt and EAF slags, probably because of their hardness, thus confirming the dependence of polishing behavior on mineralogical properties of aggregates. This result

seems to be in accordance with the data obtained from BPN measurements: those aggregates that offer lower skid resistance because of their smoothed micro-peaks as a result of the gradual removal of mineral components are also characterized by a lower density of new fragmented micro-peaks, thus resulting in lower values of *Ri* texture indicators. This "fragmentation phenomenon" that occurs during polishing causing a change of morphological characteristic of aggregates is showed in Figure 8 [34–38]. Moreover, Figure 9 shows the surface profiles before and after polishing for all types of aggregate. In particular, the gap between the black and the grey line was specifically widened to better estimate the evolution of surface microtexture on a single stone by a visual inspection.
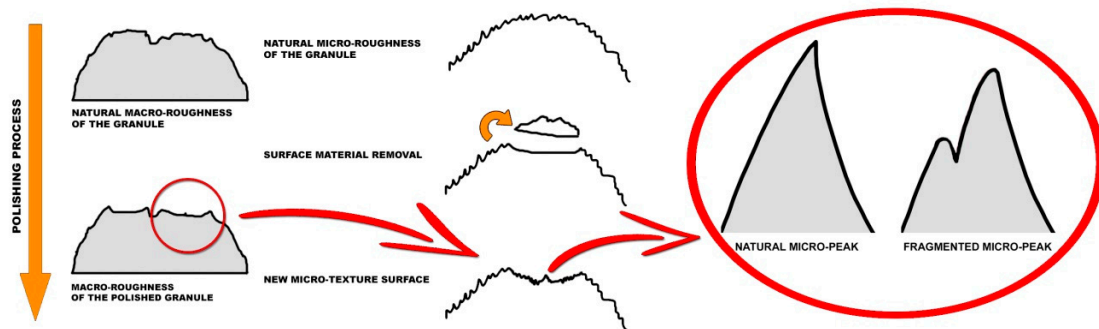

Figure 8. Schematization of fragmentation phenomenon of the aggregate surfaces under polishing procedure.
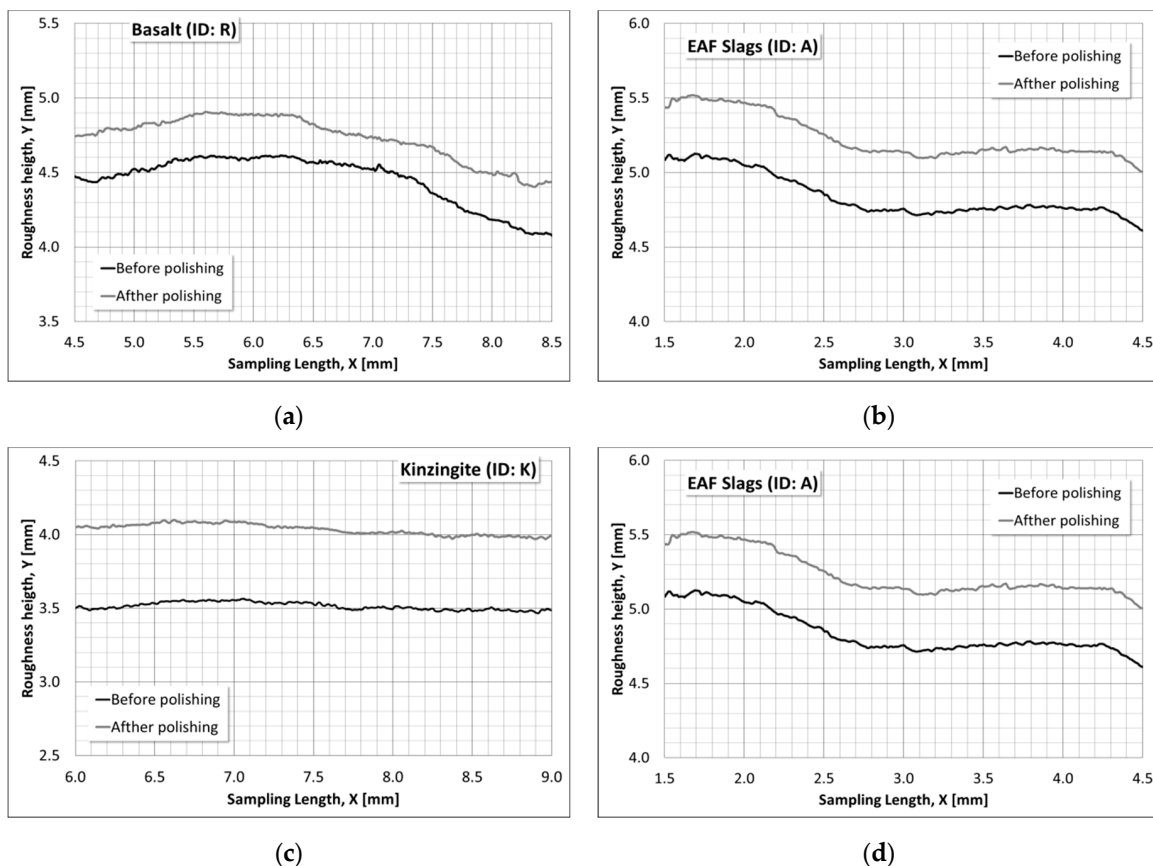

Figure 9. Examples of profile segments from the examined aggregates before and after polishing process: (**a**) basalt; (**b**) EAF Slags; (**c**) kinginzite; (**d**) limestone.

3.4. Correlations Analysis between Friction and Micro-Roughness

According to the above considerations, the correlation coefficients between friction (BPN, BPN *, and ΔBPN) and R_i (R_A, R_Q, R_Z) were carried out, Table 7 shows all correlation coefficients in term of R^2.

Table 7. Correlation coefficient R^2 between superficial friction and roughness parameters.

	BPN *	BPN	ΔBPN	R_A *	R_Q *	R_Z *	R_A	R_Q	R_Z	ΔR_A	ΔR_Q	ΔR_Z
BPN *	1	0.9341	0.7312	0.4102	0.4497	0.3722	0.5998	0.6525	0.5659	0.8102	0.7983	0.8421
BPN		1	0.9190	0.2895	0.3205	0.2502	0.4898	0.5395	0.4546	0.9066	0.9057	0.9539
ΔBPN			1	0.1668	0.1857	0.1357	0.3442	0.3822	0.3147	0.8941	0.8997	0.9453
R_A *				1	0.9963	0.9702	0.9514	0.9285	0.9399	0.2397	0.2050	0.2885
R_Q *					1	0.9695	0.9609	0.9449	0.9519	0.2651	0.2286	0.3164
R_Z *						1	0.9230	0.9012	0.9512	0.2328	0.1965	0.2616
R_A							1	0.9944	0.9845	0.4481	0.4020	0.4979
R_Q								1	0.9803	0.4890	0.4498	0.5415
R_Z									1	0.4341	0.3879	0.4737
ΔR_A										1	0.9777	0.9650
ΔR_Q											1	0.9471
ΔR_Z												1

The performance indicators marked with (*) refer to the measurements performed before polishing test.

In particular, for Table 7 it is possible to observe that roughness descriptors show high correlation coefficients between themselves in accordance with Qian and Meng [29]. R^2 values obtained by correlating BPN to roughness descriptors are always lower 0.6525 for BPN * vs. R_Q; on the contrary, very high R^2 values are registered for BPN correlation to ΔRi parameters, thus highlighting that both testing procedures (British pendulum and surface profilometric analysis) record the morphological change of aggregates characteristics due to the polishing effect (see, submatrix 3×3 top right in Table 7). The most significant correlations are shown in Figure 10a–c; from Figure 10d, it can be seen that the linear correlation between R_Q and BPN data for both polishing conditions (before, R_Q * and BPN */after, R_Q and BPN) has the same trend highlighted in previous studies [26,38], despite the R^2 value is lower than 0.6.
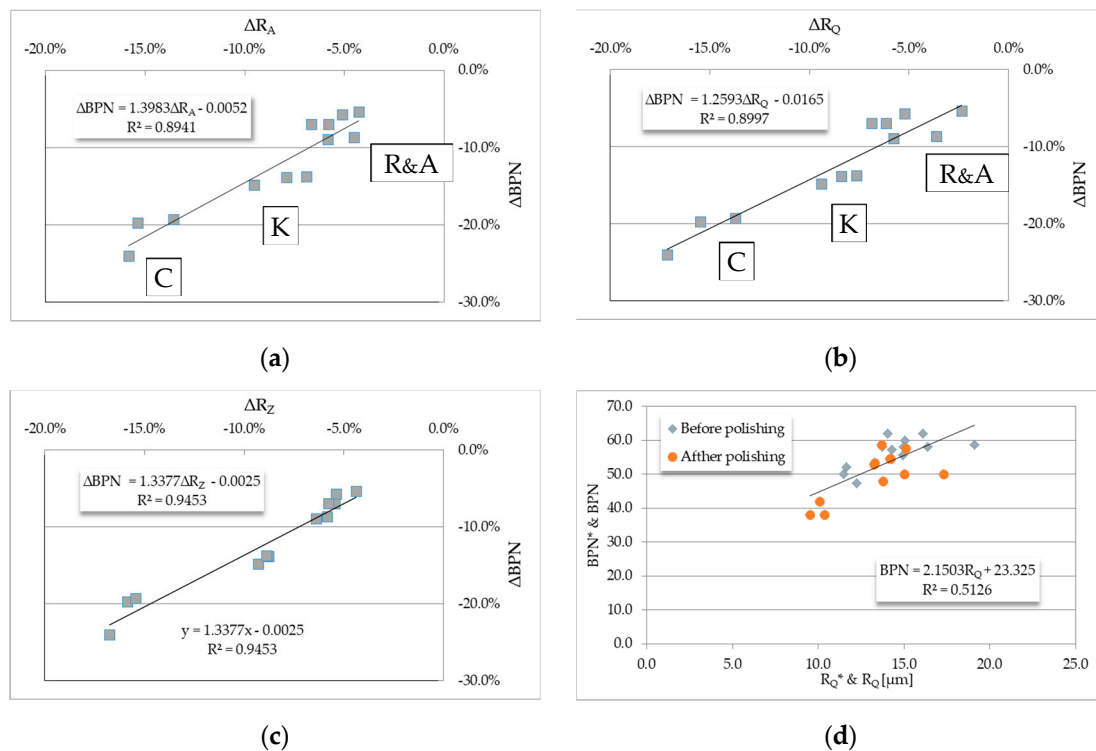

Figure 10. Relationship between percentage variations of BPN and roughness descriptors: (**a**) ΔR_A vs. ΔBPN; (**b**) ΔR_Q vs. ΔBPN; (**c**) ΔR_Z vs. ΔBPN; (**d**) R_Q * and R_Q vs. BPN * and BPN.

4. Discussion and Conclusions

This paper investigated the microtexture performance of EAF slags compared to other natural aggregates commonly used for asphalt mixes production. From experimental data analysis, the following conclusions are drawn:

- As concerns polishing resistance, PSV values registered for both EAF slags and control aggregate (basalt) are quite similar, thus confirming that steelmaking wastes offer a quite good resistance under traffic loadings;
- To confirm the above, slags behavior is quite similar to that registered for basalt aggregate also in relation to friction measurements (British pendulum number); the percentage variation of friction before/after polishing has an average value of about −7%. For the other natural aggregates double and three times higher results are registered;
- The fragmentation phenomenon that occurs on aggregate surface determines the change of aggregates morphological features. By a profilometric analysis of aggregate surface, an essentially unchanged micro-peaks configuration is registered for basalt and EAF slags, probably because of their hardness, thus confirming the dependence of polishing behavior on mineralogical properties of aggregates;
- Very high R^2 values are registered for ΔBPN correlation to ΔRi parameters, thus highlighting that both testing procedures (British pendulum and surface profilometric analysis) are sensitive to the morphological change of aggregates characteristics due to the polishing effect.

References

1. Ferreira, V.J.; Vilaplana, A.S.D.G.; Garcìa-Armigol, T.; Aranda-Usòn, A.; Lausìn-Gonzàlez, C.; Lòpez-Sabiròn, A.M.; Ferreira, G. Evaluation of the steel slag incorporation as coarse aggregate for road construction: Technical requirements and environmental impact assessment. *J. Clean. Prod.* **2009**, *130*, 175–186. [CrossRef]
2. Jiang, Y.; Ling, T.; Shi, C.; Pan, S. Characteristics of steel slags and their use in cement and concrete—A review. *Resour. Conserv. Recycl.* **2018**, *136*, 187–197. [CrossRef]
3. Dhara, S.; Kumar, S.; Roy, B.C. Management of Solid Waste for Sustainability of Steel Industry. *HCTL Open Int. J. Technol. Innov. Res. (IJTIR)* **2015**, *16*, 1–16.
4. Khunte, M. Process Waste Generation and Utilization in Steel Industry. *Int. J. Ind. Manuf. Syst. Eng.* **2018**, *3*, 1–5. [CrossRef]
5. Dash, M.K.; Patro, S.K.; Rath, A.K. Sustainable use of industrial-waste as partial replacement of fine aggregate for preparation of concrete—A review. *Int. J. Sustain. Built Environ.* **2016**, *5*, 486–516. [CrossRef]
6. Yi, H.; Xu, G.; Cheng, H.; Wang, J.; Wan, Y.; Chen, H. An overview of utilization of steel slag. In Proceedings of the 7th International Conference on Waste Management and Technology, Beijing, China, 5–7 September 2012; pp. 791–792.
7. Gelfi, M.; Cornacchia, G.; Conforti, S.; Roberti, R. Investigations on leaching behaviour of EAF steel slags. In Proceedings of the 6th European Slag Conference EUROSLAG 2010 on Ferrous Slag—Resource development for an Environmentally Sustainable World, Madrid, Spain, 20–22 October 2010; pp. 157–169.
8. Tsutsumi, N.; Kitano, Y.; Horii, K.; Kato, T.; Sugahara, K. Overview of Iron/Steel Slag Application and Development of New Utilization Technologies. *Nippon Steel Sumitomo Metal Tech. Rep.* **2015**, *109*, 5–11.

9. Aljbour, S.H.; Tarawneh, S.A.; Al-Harahsheh, A.M. Evaluation of the use of steelmaking slag as an aggregate in concrete mix: A factorial design approach. *Chem. Ind. Chem. Eng. Q.* **2017**, *23*, 113–119. [CrossRef]

10. Pellegrino, C.; Gaddo, V. Mechanical and durability characteristics of concrete containing EAF slag as aggregate. *Cem. Concr. Compos.* **2009**, *31*, 663–671. [CrossRef]

11. Xi, J.-C.; Xiang, X.-D.; Li, C.-H. Process improvement on the gradation uniformity of steel slag asphalt concrete aggregate. *Procedia Environ. Sci.* **2016**, *31*, 627–634. [CrossRef]

12. Xi, J.; Xiang, X.; Li, C. Process improvement on the gradation uniformity of steel slag asphalt concrete aggregate. In Proceedings of the Tenth International Conference on Waste Management and Technology (ICWMT), Mianyang, China, 28–30 October 2015; pp. 631–632.

13. Manso, J.M.; Gonzalez, J.J.; Polanco, J.A. Electric Arc Furnace Slag in Concrete. *J. Mater. Civ. Eng.* **2004**, *16*. [CrossRef]

14. Akinmusuru, J.O. Potential beneficial uses of steel slag wastes for civil engineering purposes. *Resour. Conserv. Recycl.* **1991**, *5*, 73–80. [CrossRef]

15. Rohde, L.; Nùnez, W.P.; Pereira Ceratti, J.A. Electric Arc Furnace Steel Slag: Base Material for Low-Volume Roads. *Transp. Res. Rec. J. Transp. Res. Board* **2003**, *1819*, 201–207. [CrossRef]

16. Shatokha, V. Environmental Sustainability of the Iron and Steel Industry: Towards Reaching the Climate Goals. *Eur. J. Sustain. Dev.* **2016**, *5*, 289–300. [CrossRef]

17. Yu, M.; Wu, G.; Kong, L.; Tang, Y. Tire-Pavement Friction Characteristics with Elastic Properties of Asphalt Pavements. *Appl. Sci.* **2017**, *7*, 1123. [CrossRef]

18. Praticò, F.G. Speed Limits and Pavement Friction: A Theoretical and Experimental Study. *Open Transp. J.* **2018**, *12*, 139–149. [CrossRef]

19. Vaiana, R.; Iuele, T.; Gallelli, V.; Rogano, D. Demanded vs Assumed friction along horizontal curves: An on-the-road experimental investigation. *J. Transp. Saf. Secur.* **2018**, *10*, 318–344. [CrossRef]

20. Li, T.; Liub, C.; Dinga, L. Impact of pavement conditions on crash severity. *Accid. Analy. Prev.* **2013**, *59*, 399–406. [CrossRef]

21. Iuele, T.; Vaiana, R.; Gallelli, V.; De Masi, F. The influence of aggregate lithological nature on pavement texture polishing: A comparative investigation on a test site in Southern Italy. *Adv. Civ. Eng. Mater.* **2016**, *5*, 337–352. [CrossRef]

22. Praticò, F.G.; Vaiana, R.; Iuele, T. Surface Performance Characterization of Single-Layer Surface Dressing: A Macrotexture Prediction Model. In *8th RILEM International Symposium on Testing and Characterization of Sustainable and Innovative Bituminous Materials*; Canestrari, F., Partl, M., Eds.; RILEM Bookseries; Springer: Dordrecht, The Netherlands, 2016; Volume 11.

23. Praticò, F.G.; Vaiana, R. A study on the relationship between mean texture depth and mean profile depth of asphalt pavements. *Constr. Build. Mater.* **2015**, *101*, 72–79. [CrossRef]

24. Praticò, F.G.; Vaiana, R.; Iuele, T. Macrotexture modeling and experimental validation for pavement surface treatments. *Constr. Build. Mater.* **2015**, *95*, 658–666. [CrossRef]

25. Cafiso, S.; Taormina, S. Texture analysis of aggregates for wearing courses in asphalt pavements. *Int. J. Pavement Eng.* **2007**, *8*, 45–54. [CrossRef]

26. Zhou, X.; Kastiukas, G.; Lantieri, C.; Tataranni, P.; Vaiana, R.; Sangiorgi, C. Mechanical and Thermal Performance of Macro-Encapsulated Phase Change Materials for Pavement Application. *Materials* **2018**, *11*, 1398. [CrossRef]

27. Praticò, F.; Vaiana, R.; Fedele, R. A study on the dependence of PEMs acoustic properties on incidence angle. *Int. J. Pavement Eng.* **2015**, *16*, 632–645. [CrossRef]

28. Boscaino, G.; Praticò, F. Classification et inventaire des indicateurs de la texture superficielle des revetements des chausses. *Bull. Lab. Ponts Chauss.* **2001**, *234*, 17–127.

29. Qian, Z.; Meng, L. Study on micro-texture and skid resistance of aggregate during polishing. *Front. Struct. Civ. Eng.* **2017**, *11*, 346–352. [CrossRef]

30. Wanga, D.; Chenb, X.; Xied, X.; Stanjekc, H.; Oesera, M.; Steinauer, B. A study of the laboratory polishing behavior of granite as road surfacing aggregate. *Constr. Build. Mater.* **2015**, *89*, 25–35. [CrossRef]

31. Ramírez, A.; Gallego, J.; Marcobal, J.R.; Blázquez, C. Development of new laboratory equipment for measuring the accelerated polishing of asphalt mixes. *Wear* **2015**, *322*, 164–170. [CrossRef]

32.　Bulevičius, M.; Petkevičius, K.; Žilionienė, D.; Drozdova, K. Testing of physical-mechanical properties of coarse aggregate, used for producing asphalt mixtures, and analysis of test results. In Proceedings of the 10th International Conference "Modern Building Materials, Structures and Techniques", Vilnius, Lithuania, 19–21 May 2010; Vainiūnas, P., Zavadskas, E.K., Eds.; Vilnius, Technika, 2010; Volume 2, pp. 1094–1098. Available online: http://dspace.vgtu.lt/bitstream/1/476/1/1094-1098_bulevicius_petkevicius_et_al.pdf (accessed on 15 May 2019).

33.　*CAPITOLATO SPECIALE DI APPALTO, Norme Tecniche, Pavimentazioni Stradali/Autostradali*; ANAS spa: Roma, Italy, 2016.

34.　Crisman, B.; Marchionna, A.; Roberti, R. Fattori Stradali da cui dipende l'aderenza. In Proceedings of the Aderenza dei Manti Bituminosi, Quaderni AIPCR/PIARC del XXIV Convegno Nazionale Stradale, Saint-Vincent, Italy, 26–29 June 2002; pp. 15–20.

35.　Wang, D.; Wang, H.; Bu, Y.; Schulze, C.; Oeser, M. Evaluation of aggregate resistance to wear with Micro-Deval test in combination with aggregate imaging techniques. *Wear* **2015**, *338*, 288–296. [CrossRef]

36.　Wang, D.; Chen, X.; Oeser, M.; Stanjek, H.; Steinauer, B. Study of micro-texture and skid resistance change of granites labs during the polishing with the Aachen Polishing Machine. *Wear* **2014**, *318*, 1–11. [CrossRef]

37.　Wang, D.; Chen, X.; Yin, C.; Oeser, M.; Steinauer, B. Influence of different polishing conditions on the skid resistance development of asphalt surface. *Wear* **2013**, *308*, 71–78. [CrossRef]

38.　Guan, B.; Wu, J.; Xie, C.; Fang, J.; Zheng, H.; Chen, H. Influence of Macrotexture and Microtexture on the Skid Resistance of Aggregates. *Adv. Mater. Sci. Eng.* **2018**, *2018*, 9. [CrossRef]